Hindawi
Journal of Engineering
Volume 2022, Article ID 3478315, 8 pages
https://doi.org/10.1155/2022/3478315

Research Article

Study on the Mechanism of Sparks Generated Mechanical Friction

He Pan[1] **and Yang Zhang**[2]

[1]*School of Mechatronic Engineering, Xuzhou College of Industrial Technology, Xuzhou 221140, China*
[2]*Jiangsu Province Xuzhou Technican Institute, Xuzhou 221000, China*

Correspondence should be addressed to He Pan; sideno311@163.com

Received 15 March 2022; Accepted 17 May 2022; Published 8 July 2022

Academic Editor: Chang-Yu Sun

In the field of explosion protection, measures must be taken to prevent ignition sources due to mechanical friction and impact. One of the most dangerous sources of ignition in methane-air mixtures is sparks, which are easily induced by friction and impact from light metals. In general, sparks and hot surfaces are coexistent in the friction processes of metal contacts. The questions are whether sparks are a truly effective ignition source and whether the nature of materials plays a decisive role in the ignition ability of sparks. Therefore, this research focuses on the temperature of hot surfaces and sparks generated by friction between pure copper, Q235A steel, and TC4 titanium alloy and the grinding wheel. The effect of the relative rotating speed on the friction temperature and friction spark characteristics is investigated. The result indicates that friction sparks are indeed easier to detonate gas than hot surfaces. Moreover, a mathematical model based on the heat transfer theory is used to prove that the sparks induced by friction from TC4 alloys are more hazardous than those induced by friction from copper and Q235A steel. The factors affecting the energy released by sparks are listed in the formula.

1. Introduction

Reducing the weight of components is one of the most effective ways to improve product properties and meet the needs of economy and ecology [1]. Lightweight components can be implemented with light shells, light space-frame structures, or mixed constructions [2]. The weight can be reduced by more than half by replacing the steel shell with a light metal shell. Bulky steel and copper materials are still widely used in explosive atmospheres [3]. Bronze, a non-sparking material, is generally used in the field of explosion protection (e.g., for hand tools) [4]. Steel materials are always applied as flameproof enclosures to isolate electrical equipment from explosive atmospheres in hazardous areas (e.g., for coal mine rescue robots) [5]. However, both copper and steel materials are too heavy to save energy. Furthermore, bulky coal mine rescue robots may result in a poor walking performance to enter the disaster site [6–10]. Therefore, lightweight construction is urgently needed. To date, replacing bulky steel and copper materials with high-strength light metal materials is an effective method to address the above problems.

Generally, titanium alloy materials have low density (about 58% of steel materials), high-temperature resistance (favorable mechanical properties at 500°C), corrosion resistance, good low-temperature performance, and good biocompatibility. Moreover, they exhibit high specific strength (3.5 times than that of stainless steel, 1.3 times than that of aluminum alloy, and 1.7 times than that of magnesium alloy). Hence, they are intensively used in aerospace, marine, chemical, weapon biological medicine, and other fields [11–13]. However, industries dealing with flammable or explosive items must take measures to prevent ignition sources due to mechanical friction and impacts [14]. Sparks and hot surfaces induced by the mechanical friction and impacts of light metal materials are the main causes for the ignition of explosive atmospheres. Maybe because of the hazard of light metal materials used in explosive atmospheres, more research studies on hot surfaces and sparks of friction and impact were focused on that of copper and

stainless-steel materials. Previous studies on hot surfaces and sparks have made the cause of ignition increasingly clear. Aluminum bronze had been shown to produce no friction sparks when the friction velocities are between 1 m/s and 20 m/s and surface pressures are between 1 N/mm^2 and 40 N/mm^2. However, hot surfaces generated by the friction of aluminum bronze had capability of igniting explosive gas [4]. Meyer et al. [15] studied the hot surfaces generated by friction contacts of five different types of steel and their effectiveness for igniting hydrogen, propane, ethylene, pentane, and diethyl ether. It was found that the effectiveness of the hot surfaces was dominated by surface-related power density not only by relative velocity. A limiting relative velocity was used to describe these ignitions in the past that had no guarantee of safety. If no sparks were generated during friction and impact, the safety of the hot surfaces could be ensured by limiting the surface-related power density [4, 15].

For impacts, Holländer et al. [16] used a torsion spring to drive the samples fixed under a hammer. The pin shape samples were made of stainless steel, and the grazing impact was performed to test their ignition ability for explosive gas. The result shows that the ignition probability increased with increasing kinetic energy. Proust et al. [17] developed a device to study the ignition of explosive atmospheres by impacts using a special "air-driven cannon" to propel a projectile accurately onto an inclined target. The results of several tests with hard steel, mild steel, bronze, pure aluminum, and quartz indicated that the relevant parameter for ignition was velocity and the nature of the material was not kinetic energy. The parameters that affect hot surfaces and sparks are dissected in increasing detail.

Then, titanium alloy materials used in explosive atmospheres, hot surfaces, and sparks would be an effective ignition source and were the sparks generated by titanium alloy more dangerous than those generated by steel and copper. The above reports did not describe the appearance and factors affecting the release of heat for sparks. Furthermore, the two points may be closely linked to the effective ignition source during the coexistence of both sparks and hot surfaces. This study aims to verify whether the titanium alloy ignites the methane-air mixture more easily than steel and copper. Hot surfaces or friction sparks would become effective ignition sources for the ethane-air mixture, and sparks of titanium alloy are more likely to be an ignition source than those of copper and steel.

2. Experiments

In order to be able to clearly observe the friction sparks at low loads and low relative speeds, the experimental setup was forged via a friction sheet that was pressed onto the rotating friction grinding wheel (Figure 1). The temperature distribution was detected by an infrared camera, and friction sparks were captured by a high-speed camera with a recording speed of 2000 frames per second. The indoor temperature was 30°C during experiments. The rotating velocity can be adjusted between 0 and 10000 n/min. The diameter of the grinding wheel was 100 cm. Experiments were carried out with three different materials that were TC4 titanium alloy, Q235A steel, and pure copper (steel and copper are safe to use in coal mines; Q235A steel is used as an impact partner to examine light alloys in the drop type testing apparatus).

3. Results and Discussion

3.1. Thermal Development of TC4, Q235A, and Cu. The temperature distribution on the surface of friction partners was clearly observed in the recording of the infrared camera, and the highest temperature appeared at the friction contact point, which increased with time and then gradually stabilized. Figure 2 shows the stable temperature distribution of the TC4 sample in the friction situation at different rotating speeds. From images 1 to 5, the rotation speed of grinding wheel is 3000 n/min (31.4 m/s), 4000 n/min (41.9 m/s), 5000 n/min (52.3 m/s), 6000 n/min (62.8 m/s), and 7000 n/min (73.2 m/s), respectively. Based on the above results, the curves of the maximum temperature of the friction area with time are shown in Figure 3. Image 6 of Figure 1 is an accidental transient high temperature that occurs during friction at a speed of 73.2 m/s. A similar instantaneous high temperature occasionally appears at different frictional speeds. The higher the speed, the higher the value has. When this sudden change in temperature occurs, the friction sparks increase instantaneously, and a clear spark explosion sound could be heard. It is presumed that the wear debris increases the instantaneous coefficient of friction. It can be explained that the friction heat ignites the small debris, increasing the friction temperature and the number of sparks. In any case, the relative speed and temperature of frictions are directly related to the generation of frictional sparks.

The friction temperatures of Q235A and Cu have similar characteristics and increase linearly with the rotating speed. Figure 4 shows the comparison of friction temperature-rotating speed curves of three materials. The friction temperature order at the same friction conditions is described as Cu > Q235A > TC4. According to the simplified equation of friction heat generation and dissipation equation,

$$q = \frac{4}{\pi}(\lambda_1 + \lambda_2)\frac{A}{R}(T - T_0), \tag{1}$$

where q is the heat generated by friction, λ is the thermal conductivity of the friction pair, A is the contact area, R is the radiation radius of the contact area, T is the temperature of the hot surface, and T_0 is the ambient temperature.

When the same frictional heat is generated, the higher the thermal conductivity is, the lower the hot surface temperature is. Then, the heat relationship between the three materials is Cu > Q235A > TC4.

Under the same friction condition, the friction heat and hot surface temperature of copper are the highest. Previous studies have shown that there is basically no friction spark when the relative velocity of friction is less than 1 m/s. If there are no friction sparks, the friction hot surfaces are the only potential ignition source. The hot surfaces generated by Cu are the most hazardous than those generated by Q235A

(a)

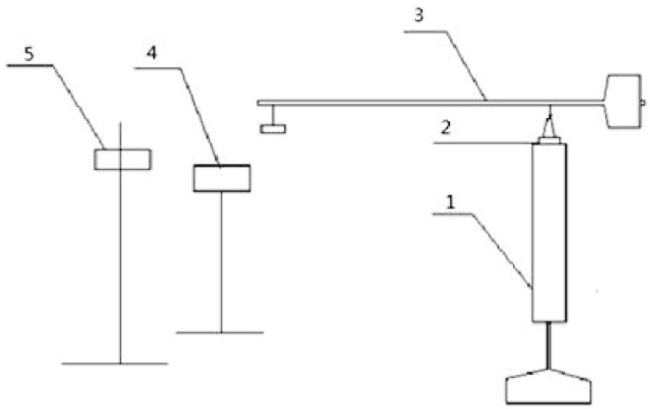

1-Variable speed grinder; 2-Sample; 3-Pressure lever; 4-Infrared video camera; 5-High-speed camera

(b)

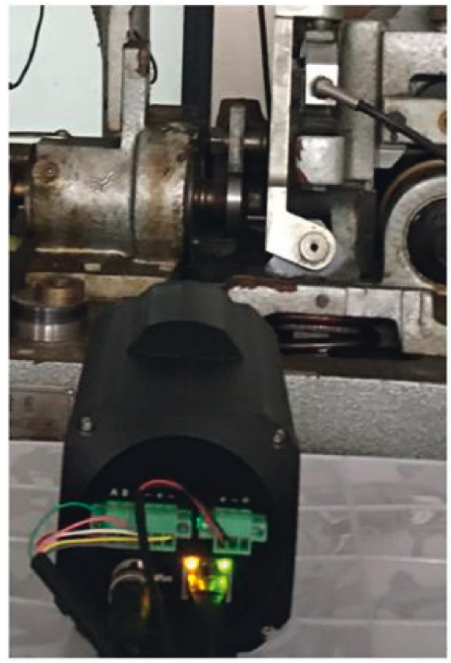

(c)

Figure 1: Experimental device schematic and photos of the experiment. (1) variable speed grinder; (2) sample; (3) pressure lever; (4) infrared video camera; (5) high-speed camera.

and TC4. Therefore, it is not comprehensive to limit the use of light metal materials in mine simply by detecting the spark safety. Similarly, a limiting relative velocity used to describe these ignitions in the past is also unreasonable. The maximum temperature of the hot surfaces is affected by the frictional relative power density and not just the frictional relative velocity. The frictional relative velocity is only one of the factors affecting the frictional relative power density.

3.2. Friction Sparks of TC4. TC4 titanium alloy cannot generate friction sparks until the grinding wheel speed exceeds 2000 n/min. At the critical speed of spark generation, friction sparks fly alongside the profile of the grinding wheel (Figure 5). Furthermore, when the relative speed increases, they fly out along with the tangent line (Figure 6). The cross arrow represents the friction contact point, a position where the sparks fly out.

With the rising rotating speed of the friction, the flight path of the sparks did not change any longer and was kept in a straight line basically (Figure 7). In order to study the characteristics of frictional sparks, the complete trajectory of two spark flights was recorded. The brightness is extremely dark when sparks are initially flying out. Due to the increasing oxidation during the flight, the sparks become bright. The sparks are extinguished or exploded and scattered into several small pieces until they disappear completely. The upper one has a smaller particle size, and the first

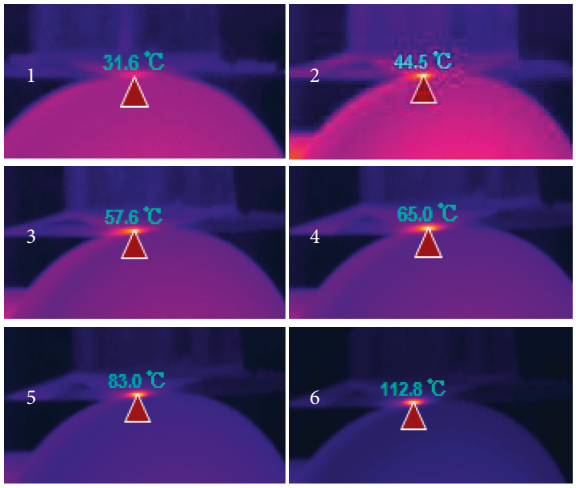

Figure 2: The temperature distribution at different speeds.

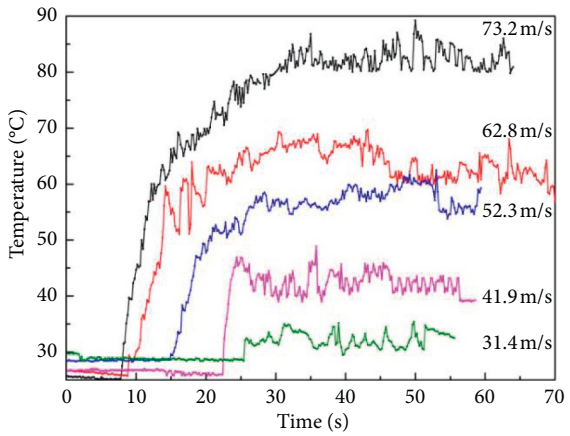

Figure 3: The temperature evolution at different speeds.

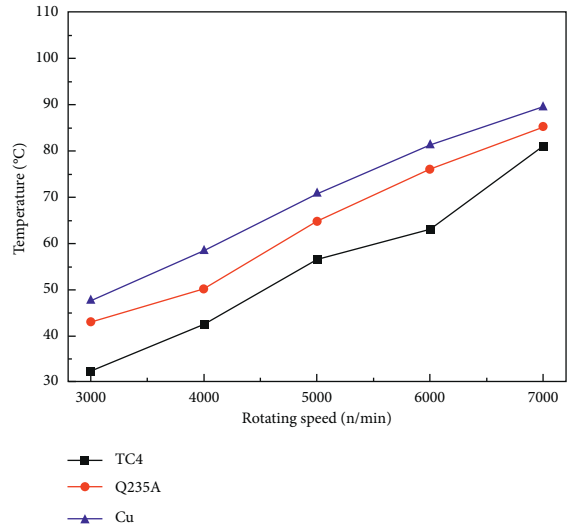

Figure 4: Temperature–speed curves of different materials.

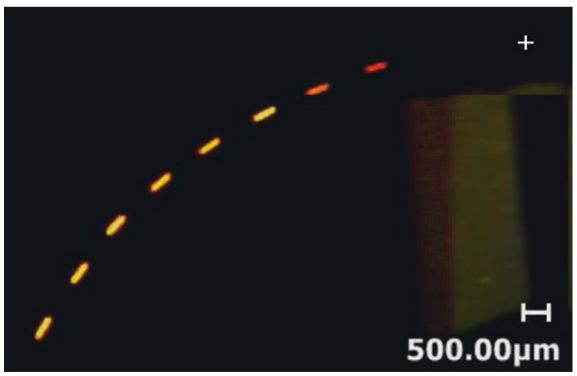

Figure 5: The spark flight path at a critical speed.

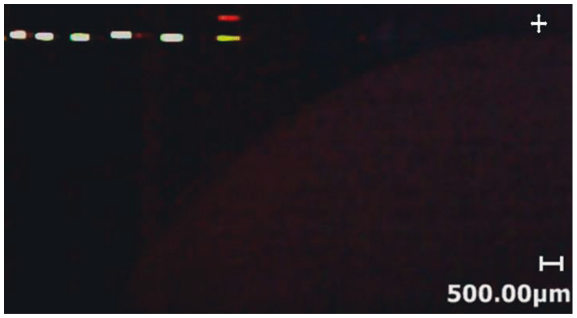

Figure 6: The spark flight path at speed of 31.4 m/s.

frame is almost invisible (Figure 7(a)). The second frame can be found, while the fourth frame disappears. The lower spark is dark at the beginning, but it becomes brighter than the upper one. Then, it becomes very bright in the second frame, and its brightness remains unchanged in the next several records. Finally, it blasts into a few darker debris in the eighth frame (Figure 7(b)). The ninth frame gradually disappears, leaving a very small dark spot (Figure 7(c)). The sparks are all flying until they either disappear or explode into tiny pieces before disappearing.

The flight path of a single set of sparks at different speeds cannot determine the law of spark flight speed. In order to identify the motion law of sparks, three sets of sparks that have longer duration at various speeds were used to measure the initial flying distance S_0 and the distance S_i of the spark flying in each frame (Table 1) and to calculate the acceleration of each segment (Table 2).

Sparks with a long distance and long duration are found under all conditions. They basically decelerate with the decreasing acceleration based on calculation. In some rare cases, the increased acceleration results in a decreased overall trend of acceleration. Similarly, the length of the spark gets shorter and shorter with the increasing flying distance in the figures of spark flight paths. It can be inferred that the particle size of sparks is small. The most critical cause affecting the flight speed is air resistance.

Based on the sparks recorded in the high-speed camera and two tables at different speed conditions, the flying distance, particle size, and brightness are not much different. But a higher speed increases the number of sparks. In order to further understand whether the flight speed of sparks is

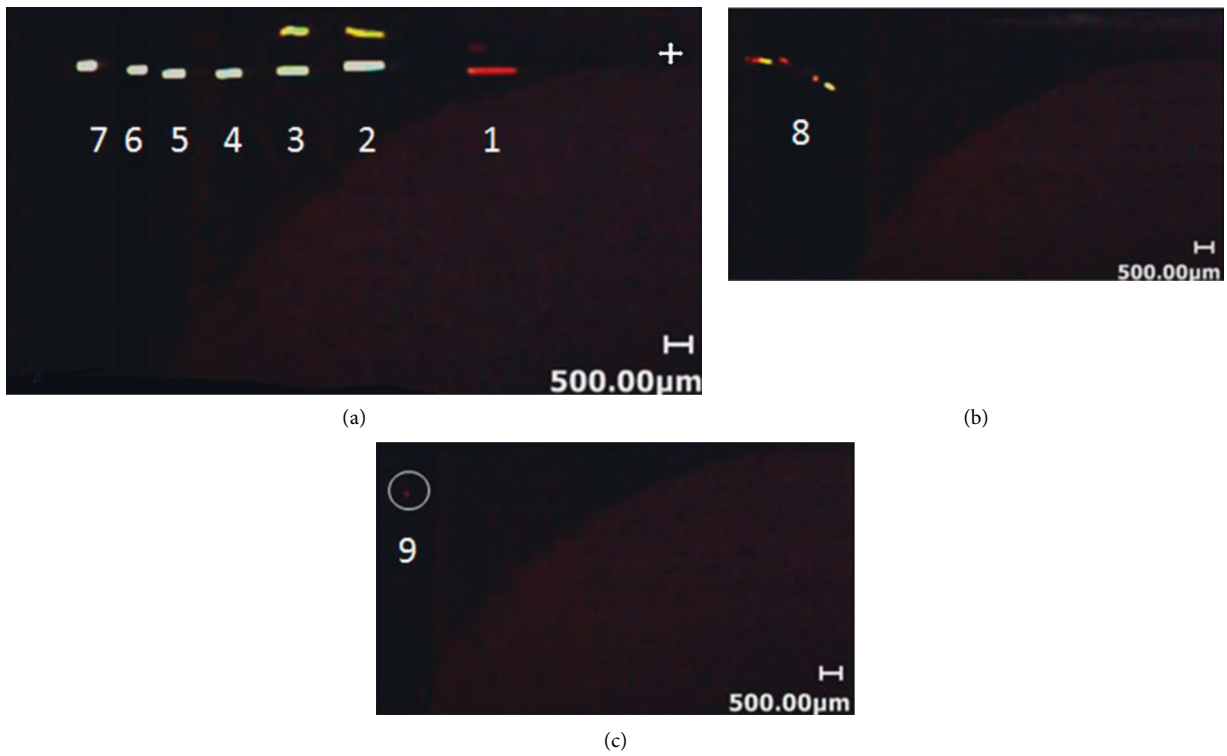

(a) (b) (c)

Figure 7: Spark flight paths at speed of 62.8 m/s.

Table 1: Measurement of the flight trajectory of TC4 sparks.

Speed (m/s)	S_0 (mm)	S_1 (mm)	S_2 (mm)	S_3 (mm	S_4 (mm)	S_5 (mm)	S_6 (mm)	S_7 (mm)	S_8 (mm)	S_9 (mm)	S_{10} (mm)
	4.5	0.85	0.775	0.7	0.65	0.55	0.5	0.45	0.4	0.35	0.3
31.4	3.25	0.75	0.65	0.55	0.45	0.35	0.3	—	—	—	—
	4.25	0.95	0.85	0.8	0.7	0.6	0.55	0.5	0.45	0.4	0.35
	4.5	1.05	0.9	0.8	0.7	0.6	0.5	0.45	0.4	0.35	0.3
41.9	3.05	1.05	0.9	0.8	0.7	0.6	0.55	0.5	0.45	0.4	0.35
	2.5	0.85	0.65	0.55	0.45	0.35	0.3	—	—	—	—
	1.75	2.15	1.4	1.15	0.9	0.75	0.65	0.55	0.45	0.4	0.35
52.3	6.25	1.6	1.3	1.05	0.9	0.8	0.7	0.6	0.5	0.45	—
	4.75	1.8	1.5	1.25	1.05	0.9	0.8	0.7	0.6	—	—
	5.75	1.35	1.1	0.9	0.75	0.6	0.5	0.45	0.4	—	—
62.8	5.5	1.5	1.2	1	0.75	0.65	0.55	0.5	0.45	0.4	—
	4	2	1.55	1.3	1.05	0.9	0.75	0.65	0.55	—	—
	6.25	1.1	0.85	0.7	0.65	0.6	0.55	—	—	—	—
73.2	2.5	1.65	1.35	1.1	0.95	0.8	0.7	0.6	0.5	—	—
	1.9	1.85	1.5	1.25	1.05	0.9	0.8	0.65	0.6	—	—

related to the speed of the grinding wheel at different speeds, 20 consecutive clear shots are selected to calculate the average speed of the flight. Table 3 provides the average speed of the fastest spark, slowest spark, and all 20 sparks. They are continuously improving with a high rotation speed of the grinding wheel (Figure 8). It can be seen that the speed of sparks is positively related to that of the grinding wheel. Moreover, the relative speed of friction has a direct impact on the speed of friction sparks.

For particle size and brightness of sparks, they are very little affected by friction conditions from the images recorded by high-speed cameras. This result is basically consistent with related research studies, and the worn particles need to have a certain size to form visible light, that is, the size of the spark is within a fixed range, not too large or too small. The average particle size of the sparks generated by TC4 is 180 μm.

3.3. Friction Sparks of Cu and Q235A. Cu generates few friction sparks. When the speed exceeds 6000 n/min, only a few sparks are taken at the beginning of the friction with contingency. Figure 9 shows the flight path of sparks of copper. The sparks are small, and the existence of time is

Table 2: Calculation of the flight trajectory TC4 sparks.

Rotate speed (m/s)	a_1 (m·s^{-2})	a_2 (m·s^{-2})	a_3 (m·s^{-2})	a_4 (m·s^{-2})	a_5 (m·s^{-2})	a_6 (m·s^{-2})	a_7 (m·s^{-2})	a_8 (m·s^{-2})	a_9 (m·s^{-2})
	300	300	300	200	200	200	200	200	200
31.4	400	400	400	400	200	—	—	—	—
	400	200	200	400	400	200	200	200	—
	600	400	400	400	400	200	200	—	—
41.9	600	400	400	400	200	200	200	-	-
	800	400	400	400	200	—	—	—	—
	3000	1000	1000	600	400	400	400	200	200
52.3	1200	1000	600	400	400	400	400	—	—
	1200	1000	800	600	400	400	400	—	—
	1000	800	600	600	400	200	200	200	—
62.8	1200	800	1000	400	400	200	200	200	—
	1800	1000	1000	600	600	400	400	—	—
	1000	600	200	200	200	200	200	—	—
73.2	1200	1000	600	400	400	400	-	—	—
	1400	1000	800	600	400	600	200	—	—

Table 3: The average flying speed of sparks at different speeds.

Grinding wheel speed (m/s)	31.4	41.9	52.3	62.8	73.2
Highest average speed (m/s)	1.6	2.0	2.4	3.87	4.11
Lowest average speed (m/s)	0.7	0.8	1.0	1.05	1.23
Average speed (m/s)	1.20	1.30	1.66	1.93	2.35

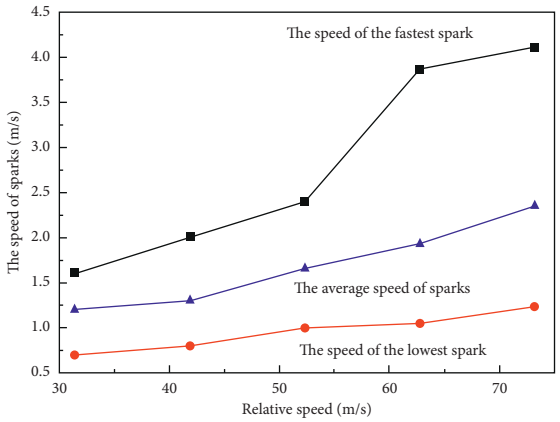

Figure 8: Relationship between spark velocity and relative friction speed.

Figure 9: The spark flight path of Cu.

extremely short. Only three frames are captured by the high-speed camera. In short, it can explain why copper has spark safety in the mine.

The sparks of Q235A are shown in Figure 10. The sparks with a longer duration are chosen. The critical speed of sparks generated by Q235A is higher. The sparks can be observed at a speed of about 2500 n/min. In fact, compared with the TC4 frictional sparks, the sparks of Q235A are darker and small and have a shorter average duration. The average distance of the initial flight is longer. Calculated in the same way as TC4 sparks, the sparks of Q235A decelerate with the decreasing acceleration. Similarly, their average speed increases with higher speed grinding-wheel. The sparks of Q235A extinguish at the end, and no explosion is observed during shooting.

Figure 10: The flight path of two frictional sparks of Q235A.

3.4. Study on the Energy Released by Sparks. The spark volume is small, and the internal thermal resistance is much smaller than the heat transfer resistance of the surface. The temperature of sparks was considered the same at the same

instant. Thus, the temperature of sparks is the only function of time and is independent of coordinates. The heat transfer between sparks and the medium can be simplified by a lumped parameter method. Then, the instantaneous heat flux of the spark is described as

$$\varnothing = \rho c V \frac{\mathrm{d}t}{\mathrm{d}\tau} = (t_s - t_0) hA \exp\left(-\frac{hA}{\rho c V}\right), \tag{2}$$

where t_s is the temperature of the spark, t_0 is the temperature of the medium, h is the convective heat transfer coefficient between the spark and medium, and ρ, c, V, and A are the density, specific heat, volume, and surface area of the spark, respectively.

If the spark duration is from 0 to τ, the total heat exchanged between the spark and the medium at this time is expressed as

$$\begin{aligned} Q &= \int_0^{\tau} \varnothing \mathrm{d}\tau = (t_s - t_0)\rho c V \left[1 - \exp\left(-\frac{hA}{\rho c V}\tau\right)\right] \\ &= \frac{4}{3}\pi \rho c r^3 (t_s - t_0)\left[1 - \exp\left(-\frac{3h}{\rho c r}\tau\right)\right]. \end{aligned} \tag{3}$$

According to the Nusselt number equation of similarity principle, h can be calculated:

$$Nu = \frac{h\ D}{\lambda}. \tag{4}$$

Assuming that the spark is a sphere and stationary, the medium flows through the sparking surface at the speed of the spark flight; the heat transfer between the spark and medium can be regarded as convective heat transfer of the outer swept ball, and then, the correlation of the fluid swept ball is

$$Nu = 2 + \left(0.4\mathrm{Re}^{1/2} + 0.6^{2/3}\right)\mathrm{Pr}^{0.4}\left(\frac{\eta_{\infty}}{\eta_w}\right)^{1/4}. \tag{5}$$

In summary, the factors affecting the release of heat can be concluded, including the density and specific heat of the material, the diameter and speed of the frictional spark, the duration of the spark combustion, and the initial temperature, thermal conductivity, kinematic viscosity, and thermal diffusivity of the medium.

The minimum detonation energy of the methane-air mixture is 0.28 mJ [18]. In the mixture of methane and air, the volume fraction of methane can be exploded when the volume fraction is 5%–16% [19]. The content of methane is not high, and the calculation parameters can be approximated with the relevant parameters of dry air. The frictional sparks of TC4 have an average diameter of 180 μm, an average speed of 1.7 m/s, and an average duration of 0.003 s (the average of one hundred sets of data, and 20 sets of different friction conditions). According to formulas (2)–(4), the temperature of the spark is calculated to be about 88°C, which may generate the detonated gas. The frictional spark of Q235A has an average diameter of 120 μm, an average speed of 1.1 m/s, and an average duration of 0.002 s. The spark temperature of 170°C can detonate the gas. The energy released from sparks of two substances could ignite the gas, and the spark temperature of Q235A is nearly twice than that of TC4. While at the same frictional conditions, the sparks of TC4 are much brighter than those of Q235A, and their temperatures are much higher than those of Q235A sparks. This can explain why steel materials are safer than TC4 as mining materials.

Previous studies [14, 16, 17] have only done a confirmatory analysis on whether sparks can ignite flammable gases. In this study, the mathematical model which calculated the energy released by sparks is deduced according to the theory of heat transfer, the main factors affecting the energy released by the spark are obtained, and the critical parameters of the spark detonation combustible gas are calculated by setting the minimum ignition energy.

4. Conclusion

The hot surfaces and sparks as potential ignition sources are generated in friction simultaneously. It is found the temperature of hot surfaces improves with the increase of the relative friction speed, while the temperature of Cu and Q235A is always higher than that of the TC4 titanium alloy. The hot surfaces generated by Cu are the most hazardous than those generated by Q235A and TC4. Consequently, simply test the spark safety of the material in explosive atmospheres, and a limiting relative velocity used to describe these ignitions in the past is considered unreasonable. For sparks, the flying speed is slightly affected by the relative rotating speed. The size and brightness of sparks are almost independent of the relative rotating speed and are more determined by the nature of materials. In short, the decisive factors in the heat released by a spark are the physical parameters of the material containing the temperature, speed and size of a spark, and physical parameters of the medium. Obviously, the key factor that affects the ignition ability of sparks is the nature of materials. The spark safety of TC4 alloy is much lower than that of copper and steel indeed.

Data Availability

The data used to support the findings of this study are included within the article.

Conflicts of Interest

The authors declare that they have no conflicts of interest.

Acknowledgments

This study was financially supported by the Joint Funds of the National Natural Science Foundation of China (U1610251) and Xuzhou Institute of Industry and Technology of High-Level Talents Scientific Research Initiation Special Project (XGY2021A044).

References

[1] M. Kleiner, M. Geiger, and A. Klaus, "Manufacturing of lightweight components by metal forming," *CIRP Annals—Manufacturing Technology*, vol. 2, no. 52, p. 521, 2003.

[2] M. Kleiner, S. Chatti, and A. Klaus, "Metal forming techniques for lightweight construction," *Journal of Materials Processing Technology*, vol. 177, p. 2, 2006.

[3] Z. Y. Song and C. Kuenzer, "Coal fires in China over the last decade: a comprehensive review," *International Journal of Coal Geology*, vol. 133, p. 72, 2014.

[4] L. Meyer, M. Thedens, and M. Beyer, "Incendivity of aluminium bronze in mechanical friction contacts," *Journal of Loss Prevention in the Process Industries*, vol. 49, p. 947, 2017.

[5] T. Krause, J. Bewersdorff, and D. Markus, "Investigations of static and dynamic stresses of flameproof enclosures," *Journal of Loss Prevention in the Process Industries*, vol. 49, p. 775, 2017.

[6] A. Morris, D. Ferguson, Z. Omohundro et al., "Recent developments in subterranean robotics," *Journal of Field Robotics*, vol. 23, no. 1, p. 35, 2006.

[7] J. C. Zhao, J. Y. Gao, F. Z. Zhao, and Y. Liu, "A search-and-rescue robot system for remotely sensing the underground coal mine environment," *Sensors*, vol. 17, no. 10, Article ID 2426, 2017.

[8] W. D. Wang, W. Dong, Y. Y. Su, D. M. Wu, and Z. J. Du, "Development of search-and-rescue robots for underground coal mine applications," *Journal of Field Robotics*, vol. 31, no. 3, p. 386, 2014.

[9] Y. T. Li, H. Zhu, M. G. Li, and P. Li, "A novel explosion-proof walking system: twin dual-motor drive tracked units for coal mine rescue robots," *Journal of Central South University*, vol. 23, no. 10, Article ID 2570, 2016.

[10] Y. T. Li and H. Zhu, "A simple optimization method for the design of a lightweight, explosion-proof housing for a coal mine rescue robot," *Journal of the Brazilian Society of Mechanical Sciences and Engineering*, vol. 40, no. 340, p. 2, 2018.

[11] B. Dipankar and J. C. Williams, "Perspectives on titanium science and Technology," *Acta Materialia*, vol. 61, p. 844, 2013.

[12] H. Clemens and W. Smarsly, "Light-weight intermetallic titanium aluminides-status of research and development," *Advanced Materials Research*, vol. 278, p. 551, 2011.

[13] R. Pflumm, S. Friedle, and M. Schütze, "Oxidation protection of γ-TiAl-based alloys-A review," *Intermetallics*, vol. 56, pp. 1–14, 2015.

[14] T. Komai, S. Uchida, and M. Umezu, "Ignition of methane-air mixture by frictional sparks from light alloys," *Safety Science*, vol. 17, no. 2, p. 91, 1994.

[15] L. Meyer, M. Beyer, and U. Krause, "Hot surfaces generated by sliding metal contacts and their effectiveness as an ignition source," *Journal of Loss Prevention in the Process Industries*, vol. 36, p. 532, 2015.

[16] L. Holländer, T. Grunewald, and R. Grätz, "Influence of material properties of stainless steel on the ignition probability of flammable gas mixtures due to mechanical impacts," *Chemical Engineering Transactions*, vol. 48, p. 307, 2016.

[17] C. Proust, S. Hawksworth, R. Rogers et al., "Development of a method for predicting the ignition of explosive atmospheres by mechanical friction and impacts (MECHEX)," *Journal of Loss Prevention in the Process Industries*, vol. 20, p. 349, 2007.

[18] J. L. Xu, S. H. Zhang, H. W. Jin, and Z. H. Li, "Experimental study on gas explosion detonated by the tensile failure sparks of anchor rope," *China Safety Science Journal*, vol. 2, no. 14, p. 3, 2004.

[19] Z. W. Qu, *Research on Flammability Limit and Quenching Mechanism of Flame of Premixed Methane Gas*, Anhui University of Science and Technilogy, Anhui, China, 2015.